



AUTHOR(S):

TITLE:

YEAR:

Publisher citation:

OpenAIR citation:

Publisher copyright statement:

This is the _____ version of an article originally published by _____
in _____
(ISSN _____; eISSN _____).

OpenAIR takedown statement:

Section 6 of the "Repository policy for OpenAIR @ RGU" (available from <http://www.rgu.ac.uk/staff-and-current-students/library/library-policies/repository-policies>) provides guidance on the criteria under which RGU will consider withdrawing material from OpenAIR. If you believe that this item is subject to any of these criteria, or for any other reason should not be held on OpenAIR, then please contact openair-help@rgu.ac.uk with the details of the item and the nature of your complaint.

This publication is distributed under a CC _____ license.

Efficient Wireless Multimedia Multicast in Multi-rate Multi-channel Mesh Networks

Wanqing Tu

Department of Computing Science, The Robert Gordon University, Aberdeen, UK.

Email: w.tu@rgu.ac.uk

Abstract—Devices in wireless mesh networks can operate on multiple channels and automatically adjust their transmission rates for the occupied channels. This paper shows how to improve performance-guaranteed multicasting transmission coverage for wireless multi-hop mesh networks by exploring the transmission opportunity offered by multiple rates (MR) and multiple channels (MC). Based on the characteristics of transmissions with different rates, we propose and analyze parallel low-rate transmissions (PLT) and alternative rate transmissions (ART) to explore the advantages of MRMC in improving the performance and coverage tradeoff under the constraint of limited channel resources. We then apply these new transmission schemes to improving the WMN multicast experience. Combined with the strategy of reliable interference-controlled connections, a novel MRMC multicast algorithm (LC-MRMC) is designed to make efficient use of channel and rate resources to greatly extend wireless multicast coverage with high throughput and short delay performance. Our NS2 simulation results prove that ART and LC-MRMC achieve improved wireless transmission quality across much larger areas as compared to other related studies.

Index Terms—Wireless multicasting, multiple rates, multiple channels, wireless mesh networks.

I. INTRODUCTION

Multicast in wireless mesh networks (WMN) is promising in efficiently utilizing wireless resources to provide flexible and reliable wireless connections to a group of multimedia receivers (e.g., video conferencing users). However, as illustrated in Fig. 1, wireless multicasting leads to complicated interference patterns for the following reasons.

- 1) Consecutive transmissions on the same multi-hop WMN paths. In Fig. 1 (a), on the multicasting path $n_0 \rightarrow n_1 \rightarrow n_2$, because of the streaming transmission of multimedia data, while n_0 sends the multicasting traffic to n_1 , n_1 is forwarding multicast data (received from n_0) to n_2 . Due to the nature of wireless broadcast, as highlighted in the circle of Fig. 1 (a), the transmission $n_1 \rightarrow n_2$ competes with the transmission $n_0 \rightarrow n_1$ to occupy the same channel. This conflict degrades the multicast performance from n_0 to n_1 as well as from n_1 to n_2 ;
- 2) Parallel delivery of multicast data on paths that have at least one interfering hop. In Fig. 1 (b), suppose n_1 and n_3 are within each other's interfering range. While multicasting transmissions are on the path $n_0 \rightarrow n_1 \rightarrow n_2$, multicasting transmissions $n_3 \rightarrow n_4$ take place in parallel. The parallel transmissions on these paths cause interference (shown in the circle of Fig. 1 (b)) which further degrades the performance of multimedia traffic entering n_1 and n_3 .

The above interference becomes more intensive when multicasting multimedia data because of the high transmission rates and the long communication durations. Multimedia performance is hence degraded quickly during wireless multicasting transmissions, limiting the distances across which users can join the applications with guaranteed performance.

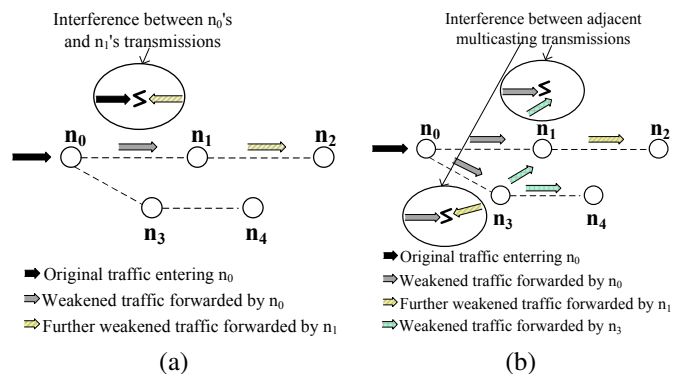


Fig. 1. An example of wireless multicasting interference.

One line of study to address this complicated interference is to employ multiple orthogonal (i.e., non-overlapping) channels at interfering nodes. By attaching orthogonal channels to different radio interfaces, the non-interfering capacity of a WMN may be increased. In the literature, orthogonal channels are utilized either in parallel at single nodes to achieve a great accumulated capacity or at successive nodes in series to effectively avoid interfering transmissions. However, with current wireless technology, there is a limited number of orthogonal channels that are not sufficient for multihop WMN multicast because interference caused by the rich connectivity is substantial. Hence, it is difficult to gain significant improvement in extending performance-guaranteed multicast coverage by only efficiently using orthogonal channels.

Apart from operating on multiple channels, WMN devices (i.e., gateways, routers, or client nodes) can also adjust their transmission rates freely whenever necessary. With the availability of multiple transmission rates, WMN communication performance can be improved either by detouring around bottleneck or interfering nodes or by referring to network conditions to determine an appropriate transmission rate. However, the employment of multiple transmission rates in a WMN multimedia multicast may easily cause a very complicated interference topology. This is because different transmission rates have different coverage - an adaptive change of a

transmission rate may incur new interference on a structured multicast tree.

As above, research has been carried out to exploit multiple transmission rates (MRs) or multiple channels (MCs) separately. Few studies proposed to explore the advantages of combining multiple channels and multiple rates, mainly focusing on improving communication performance such as delays [11], transmission rates [12], etc. With the popularity of portable multimedia end-user devices (e.g., smart phones, tablet pcs, mobile gaming terminals), the number of online users is rapidly increasing and these users spread across wider and wider areas, posing a new challenge which is to employ limited channel resources to scalably multicast high-performance multimedia traffic in a multi-hop WMN. Being rarely involved in previous studies, this paper tackles the challenge by combining MRs and MCs to explore transmission opportunitiess in improving performance-guaranteed multimedia multicasting transmission distance for multi-hop WMNs. More specifically, based on the characteristics of and the obstacles experienced by MRMC wireless transmissions, we present the following contributions in this paper.

- *The parallel low-rate transmission* scheme (PLT) improves performance-guaranteed wireless coverage by simply equipping a mesh node with multiple channels transmitting at a rate lower than the maximum available rate in parallel. As such, an aggregated throughput higher than that of the maximum available rate can be achieved across greater distances. As compared to our study that develops PLT theoretically in a unicast WMN [18], this paper not only concerns PLT in a multicast WMN but also develops the implementation details of PLT in order to efficiently integrate with the underlying hardware (i.e., radio interfaces) and protocols (e.g., TCP/UDP).
- *The alternative rate transmission* algorithm (ART) makes efficient use of limited channels and transmission rates to achieve great high-performance wireless communication coverage by 1) alternatively employing PLT transmissions (with the PLT transmission rate) at the $j(\lceil \frac{\tilde{\mu}}{d} \rceil + 1)$ th¹ hops and regular transmissions (with the benchmark transmission rate) at other hops, where $j \in N$, d is the radius of the transmission range of the benchmark rate and $\tilde{\mu}$ is the radius of the interference range of the PLT rate, and 2) selecting appropriate benchmark and PLT rates to provide the best balance between performance and coverage under conditions of limited channel diversity.
- *The link-controlled multi-rate multi-channel multicast* algorithm (LC-MRMC) improves our previous work [18] by focusing on a WMN with multiple multicasting groups. The enhanced LC-MRMC algorithm builds a multicast tree, shared by coexisting groups, that hires the minimum number of WMN nodes to implement reliable ART transmissions while greatly controlling multicast interference. As such, wireless multicast coverage with high throughput and short delays is greatly extended.

¹In this paper, we use the symbol $\lceil \bullet \rceil$ to represent the smallest integer greater than \bullet .

The paper is organized as follows. Section II overviews related studies. Sections III and IV propose the novel PLT and ART transmission schemes respectively. Section V designs the LC-MRMC algorithm. Section VI presents our NS2 simulation studies. Section VII concludes the paper.

II. RELATED WORK

Multi-channel multi-radio multicast. Research on multiple channels has consistently focused on channel assignment with diverse static and dynamic solutions being proposed. O. Karimi *et al.* [1] studied high-throughput WMN multicast by exploring the advantages of channel diversity and multiple mesh gateways. By forming WMN multicast as a mathematical problem, an iterative primal-dual optimization framework is proposed to iteratively switch between solving primal sub-problems for channel allocation and routing. S. Lim *et al.* [2] improved multicast connectivity in a multi-channel WMN. The proposed protocol builds multicasting paths while inviting multicast members. The channel assignment guarantees that neighboring members will have common channels. N. Lan *et al.* [3] presented a channel assignment algorithm that uses both orthogonal and overlapping channels to minimize interference for WMN multicast. H. Chiu *et al.* [4] proposed an integer linear program and an associated heuristic algorithm for WMN multicast to efficiently minimize the carried load on the most-heavily loaded channel and maximize the residual capacity of the most heavily loaded node by using multiple channels.

Multi-rate multicast. Research on multiple transmission rates has investigated rate adaption and rate allocation schemes. J. Choi *et al.* [5] presented algorithms to dynamically control wireless transmission rates based on collision situations. H. Zhu *et al.* [6] proposed to adjust transmission rates by referring to the signal to noise ratio that can be achieved by exchanging control messages. T. Kim *et al.* [7] studied rate adaption on a per path basis. A new metric ETM is studied that takes the relative position of a link on a path and the avoidance of congestion areas into account to adjust transmission rates for WMN routing to achieve reliably high throughput. A. Kakhbod *et al.* [8] considered the decentralized bandwidth/rate allocation problem in multi-rate multicast service provisioning with strategic users. O. Alay *et al.* [9] proposed a method to dynamically adapt the transmission rate and Forward Error Correction (FEC) for video multicast over multi-rate wireless networks.

Multi-channel multi-rate multicast. The advantages of multiple rates and multiple channels in combination have also been explored in the literature. S. Bodas *et al.* [10] studied scheduling algorithms for multi-channel OFDM-based down-link systems. A Markov chain mathematical technique that improves on traditional ON-OFF models is developed for channels with multiple rates. K. Lee *et al.* [23] proposed rate-controlled parallel transmissions to improve the QoS of multimedia connections as well as allocate resources efficiently. This is achieved by decomposing the available radio resources into multiple sets of links with different levels of reliability. Different layers of a multimedia stream with different levels of importance are then sent over a wireless channel that supports multiple links with heterogeneous reliability. For

MRMC in WMNs, J. Qadir *et al.* [11] designed degree-free (DF) transmissions. L. Farzinshah *et al.* [12] used MRMC to handle the bandwidth heterogeneity of multicast receivers. A multi-gateway multi-rate multicast routing scheme was developed to maximize the total achieved data rates at receivers while preserving fairness between them. To the best of our knowledge, the structured DF scheme is the most closely related to our study motivations. Hence, we further develop the introduction to DF below.

DF was designed for WMN broadcasting to achieve short latency performance. It allows a DF node to employ multiple channels transmitting at different rates. Each channel sets up a connection between this DF node and its downstream neighbor(s) that cannot be covered by a transmission rate larger than the employed rate of this channel. In this way, mesh nodes are not required to compromise by accepting a lower quality of service to accommodate more distant nodes which may receive at a lower rate with longer delays. Instead, DF delivers traffic multiple times via channels with different rates which enables closer nodes to receive data with shorter delays (because of a faster transmission rate). DF may be effective when network traffic load is light. However, it may not suit high-rate multimedia communications because multiple DF transmissions of the same high-rate traffic easily causes bottleneck nodes. We are hence motivated to develop a new MRMC study that can efficiently utilize communication resources to achieve the goal of extending performance-guaranteed coverage.

III. PARALLEL LOW-RATE TRANSMISSION (PLT)

A. Throughput-coverage Tradeoff

It has been established in the literature that a tradeoff exists between improving network throughput and extending transmission coverage. Generally, for a channel transmitting at a higher rate, a higher communication throughput is delivered to a smaller area. This tradeoff becomes severe in a multicast communication as shown by the following example.

We consider a simple IEEE 802.11b wireless multicast in Fig. 2. Suppose n_1 is located in the 11Mbps transmission range of n_0 and n_2 is located out of the 11Mbps transmission range but within the 5.5Mbps transmission range of n_0 . In the literature, it is not unusual for n_0 to transmit at 5.5Mbps for the sake of connectivity. However, this limits the throughput and prolongs the delays that n_1 can potentially achieve since n_0 is capable of transmitting at 11Mbps. Moreover, when n_1 forwards the received packets to n_3 , the already degraded throughput or delays at n_1 may cause unacceptable performance at n_3 if n_3 requires at least 5.5Mbps throughput. This shrinks multicast coverage when n_3 cannot be admitted into the multicast.

Degree-Free Transmissions (DF) [11]² employ multiple channels and multiple rates to address the above tradeoff. As shown in Fig. 2 (a), DF enables n_0 to be equipped with two channels - one for transmissions at 11Mbps (to n_1) and the other for transmissions at 5.5Mbps (to n_2). In this way, n_1 can achieve throughput or delays as great as its connection allows and n_3 can be admitted to the multicast

with acceptable performance via the third channel. However, DF inefficiently utilizes resources (e.g., node power, channel bandwidth) as n_0 has to schedule the transmission of the same information twice. In a more complicated topology, when a node has several direct children, this node could easily become a bottleneck in a DF multimedia multicast affecting both performance and coverage of the multicast.

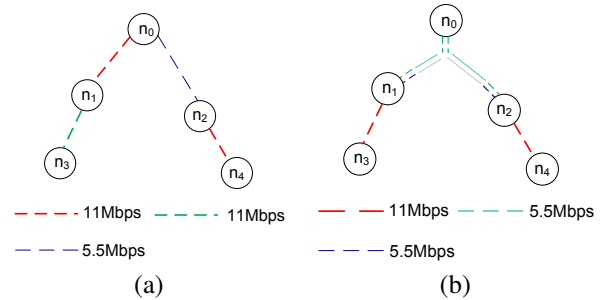


Fig. 2. An example of wireless multicast with DF (a) and with PLT (b).

B. Parallel Low-rate Transmissions (PLT)

In order to efficiently utilize MRMC to extend performance-guaranteed multicasting coverage via simple and low-overhead operations, we propose the idea of parallel low-rate transmissions (PLT). Instead of hiring multiple channels working at different rates to transmit a multimedia stream multiple times to guarantee the maximum available throughput for different receivers, PLT employs multiple channels to transmit a multimedia stream together and at the same rate, this being less than the maximum available rate. In other words, through multiple low-rate channels, PLT provides an aggregate high throughput to users across a larger area. We use a simple example in Fig. 2 (b) to illustrate PLT. As a PLT node, n_0 employs two 5.5Mbps orthogonal channels in parallel to transmit half of the traffic via each channel. As a result, both n_1 and n_2 receive the same high network throughput without requiring n_0 to transmit the same traffic more than once. Like DF, in this multicast, PLT uses 3 orthogonal channels.

To maximize transmission coverage, ideally, a PLT node multicasts at the minimum available rate r_{min} . This means that, to achieve the best throughput performance, the number of channels employed in parallel by the PLT node is $\lceil \frac{r_{max}}{r_{min}} \rceil$. However, there is a limited number of orthogonal channels which may not always be sufficient to offer the required $\lceil \frac{r_{max}}{r_{min}} \rceil$ channels. Thus, in Section IV. B, we will study an appropriate PLT rate r ($r_{min} \leq r \leq r_{max}$) under the constraint of channel diversity.

The implementation of PLT requires the splitting of a full multimedia stream into $\lceil \frac{r_{max}}{r} \rceil$ subflows. These subflows are multicasted to next-hop nodes via $\lceil \frac{r_{max}}{r} \rceil$ different channels in parallel. More specifically, PLT nodes switch a single radio interface between $\lceil \frac{r_{max}}{r} \rceil$ channels to multicast or receive $\lceil \frac{r_{max}}{r} \rceil$ subflows. As illustrated by the blue switched connections in Fig. 3, n_0 hops between different channels via its radio interface to multicast data to n_1 and n_3 , and n_1 and n_3 receive multimedia data from these channels in the same

²Please refer to Section II for our introduction to DF.

round robin fashion as n_0 . Since all PLT channels use the same transmission rate, the splitting of the multimedia stream is accomplished by simply scheduling packets to be transmitted via different channels in a round robin fashion. In this way, PLT nodes can also switch their radio interfaces between adopted orthogonal channels. Such scheduling allows multiple channels to share traffic load via a single radio interface with little overhead or additional processing. Furthermore, when a PLT node has sufficient radio interfaces for sending or receiving, $\lceil \frac{r_{max}}{r} \rceil$ channels can transmit simultaneously and so do not need to connect to a radio interface in turn. The practical implementation of the round robin schedule should take the clock skew between different nodes into account. A number of studies have proposed useful schemes (e.g., the Network Time Protocol) to distributively address the clock skew which can be easily adopted by PLT nodes.

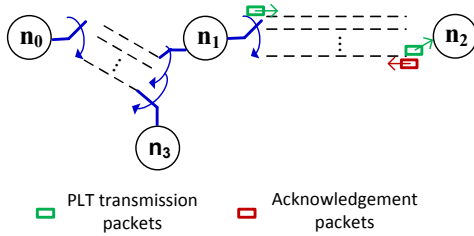


Fig. 3. An example of PLT transmissions.

Round robin PLT transmissions can be applied with the TCP protocol (e.g., the application of web streaming) or the UDP protocol (e.g., the application of video conferencing). UDP does not recover lost packets. However, with TCP, a PLT multicast receiver is required to retransmit lost packets when it detects packet loss. In order to facilitate fast loss recovery, each PLT multicasting forwarder caches multicasting packets for a period of time equal to the transmission delay from the forwarder to its downstream receivers³. If this forwarder connects to its different downstream receivers with different delays, the longest delay is used as the packet caching time. A PLT multicast receiver reports packet loss through a multi-hop return path, reversing the direction from which packets come to the receiver. The TCP acknowledgement uses the channel that has most recently received a packet. For example, in Fig. 3, if n_2 detects a packet loss while it receives a packet (shown by the green box) from the bottom channel, n_2 reports a packet acknowledging a packet loss (shown by the red box) back toward n_0 via its bottom channel. At each hop on the return path,

- if a forwarder has dropped the requested packet(s) from its cache, this forwarder continues forwarding the TCP acknowledgement by using the channel that has most recently received a packet. This benefits fast loss recovery while incurring the least interruption to the PLT multicast of the sender. This is because a channel that has just completed sending a packet in round robin PLT will have some availability until it is scheduled for round robin

once more, and so it has greater opportunity to send a TCP message back;

- otherwise if a forwarder still has the requested packet(s), it stops circulating the TCP acknowledgement but retransmits the requested packet(s) to the receiver if the packet(s) can arrive at the receiver(s) before the scheduled representation time of the packet(s)⁴. The forwarder transmits retransmitted packets with priority via the next available channel.

C. Analysis of PLT

We now theoretically evaluate the two transmission schemes (PLT and DF), considering an interference model concerning transmissions on the same channel with receivers of one transmission within the interference range of another transmission. Suppose there are n ($n > 0$) different rates, denoted as $\{r_0, r_1, \dots, r_{n-1}\}$, required by DF. Based on the studies in [18-20], due to MAC overheads, the throughput provided by a transmission rate is reduced from the nominal transmission rate. For example, a 11Mbps transmission may only provide 4.55Mbps throughput to its next-hop receiver(s) [18-19]. Without loss of generality, we denote the throughput reduction factor of rate r_i ($i \in [0, n-1]$) as β_i . Meanwhile, we use d_i to represent the radius of transmission range of rate r_i and μ_i to represent the radius of interference range of rate r_i . For PLT, if its transmission rate is r ($r_{min} \leq r \leq r_{max}$), denote the throughput reduction factor of r as β and the radii of transmission range and interference range of rate r as d and μ , where $r_{max} = \max\{r_i, i \in [0, n-1]\}$ and $r_{min} = \min\{r_i, i \in [0, n-1]\}$.

Theorem 1 For a WMN node that multicasts data to a group of receivers, PLT overtakes DF in terms of average throughput by at least $\frac{\min\{R, \beta_{n-1} r_{n-1} p^{PLT}\} d_{n-1}^2 \lceil \frac{r_0}{r_{n-1}} \rceil}{d_0^2 \min\{R, \beta_0 r_0 p^{DF}\} + \sum_{i=1}^{n-1} (d_i^2 - d_{i-1}^2) \min\{R, \beta_i r_i p^{DF}\}} - 1$, where d_i is the radius of transmission range of rate r_i ($i \in [0, n-1]$), r_i is the i th transmission rate used by DF, R is the traffic load of the multicasting transmission, $p^{DF} = p^{PLT}$ represents the transmission probability of a multicasting node via the channel with rate r_{n-1} .

Proof. For a DF multicast node, suppose it needs n channels to cover all its multicast receivers. In order to provide the greatest throughput that these receivers can attain, each of these n channels transmits at a different rate. Denote the set of rates as $\{r_0, r_1, \dots, r_{n-1}\}$ and assume $r_i \geq r_j$ if $j \geq i$ ($i, j \in [0, n-1]$). Without loss of generality, suppose nodes in an interference range have the same priority to occupy a channel, then the transmission probability of the DF multicast node via channel i is $p_i^{DF} = \frac{1}{\pi \mu_i^2 \eta}$, where η is the average distribution density of WMN nodes and μ_i is the radius of interference range of rate r_i . When $r_i \geq r_j$, the interference range of the channel with r_i is smaller than the interference range of the channel with r_j , i.e., $p_i^{DF} \geq p_j^{DF}$ as a larger coverage experiences a higher interference possibility. To synchronize data delivery to downstream neighbors via n channels, the DF node should transmit with the probability

³There are quite a few studies in the literature that can facilitate PLT (e.g., [17]) to achieve end-to-end delays.

⁴ The representation time of a lost packet can be included in the TCP message issued to the sender.

(p^{DF}) equal to the minimum transmission probability among n channels (i.e., the transmission probability of the channel with r_{min}). This means that the achievable throughput of a channel transmitting at r_i is at most $\min\{R, \beta_i r_i p^{DF}\}$, where R is the traffic load of the multicasting transmission.

We now consider the number of users who can achieve this throughput $\min\{R, \beta_i r_i p^{DF}\}$ based on the average node distribution density η . For the rate r_0 , the throughput $\min\{R, \beta_0 r_0 p^{DF}\}$ is received by users located in the transmission range of r_0 . For the rate r_i ($0 < i \leq n-1$), the throughput $\min\{R, \beta_i r_i p^{DF}\}$ is received by users located in the transmission range of r_i but outside of the transmission range of r_{i-1} (i.e., the rate immediately larger than r_i). Therefore, the total number of users receiving $\min\{R, \beta_0 r_0 p^{DF}\}$ is $\pi d_0^2 \eta$ and the total number of users receiving $\min\{R, \beta_i r_i p^{DF}\}$ is $\pi(d_i^2 - d_{i-1}^2)\eta$, where d_{i-1} and d_i are the radiuses of transmission range of r_{i-1} and r_i respectively. Hence, the average throughput of DF is

$$T_D = \frac{\pi d_0^2 \eta \min\{R, \beta_0 r_0 p^{DF}\}}{\pi d_{n-1}^2 \eta} + \frac{\sum_{i=1}^{n-1} \pi(d_i^2 - d_{i-1}^2) \eta \min\{R, \beta_i r_i p^{DF}\}}{\pi d_{n-1}^2 \eta}.$$

For the PLT transmission, if the lowest rate r_{n-1} is employed for extending the coverage, a number of $\lceil \frac{r_0}{r_{n-1}} \rceil$ channels⁵ should be employed in parallel in order to make up the throughput difference between r_0 and r_{n-1} . Then, the average throughput of all PLT receivers is

$$T_P = \frac{\pi d_{n-1}^2 \eta \lceil \frac{r_0}{r_{n-1}} \rceil \min\{R, \beta_{n-1} r_{n-1} p^{PLT}\}}{\pi d_{n-1}^2 \eta} = \lceil \frac{r_0}{r_{n-1}} \rceil \min\{R, \beta_{n-1} r_{n-1} p^{PLT}\}.$$

To compare the two transmission schemes, if $r_j < r_i$ ($j \in [0, n-1], j \neq i$), $\beta_j r_j < \beta_i r_i$ which means $\min\{R, \beta_0 r_0 p^{DF}\} \geq \min\{R, \beta_i r_i p^{DF}\}$, we have

$$\frac{d_0^2 \min\{R, \beta_0 r_0 p^{DF}\} + \sum_{i=1}^{n-1} (d_i^2 - d_{i-1}^2) \min\{R, \beta_i r_i p^{DF}\}}{d_{n-1}^2 \lceil \frac{r_0}{r_{n-1}} \rceil \min\{R, \beta_{n-1} r_{n-1} p^{PLT}\}} \leq \frac{\min\{R, \beta_0 r_0 p^{DF}\} [d_0^2 + \sum_{i=1}^{n-1} (d_i^2 - d_{i-1}^2)]}{\min\{R, \beta_{n-1} r_{n-1} p^{PLT}\} d_{n-1}^2 \lceil \frac{r_0}{r_{n-1}} \rceil} \quad (1)$$

When $R \leq \beta_{n-1} r_{n-1} p^{PLT}$, expression (1) can be simplified to $\frac{d_0^2 + \sum_{i=1}^{n-1} (d_i^2 - d_{i-1}^2)}{d_{n-1}^2 \lceil \frac{r_0}{r_{n-1}} \rceil} = \frac{1}{\lceil \frac{r_0}{r_{n-1}} \rceil} < 1$; when $R \geq \beta_0 r_0 p^{DF}$, expression (1) can be simplified to $\frac{\beta_0 r_0 p^{DF}}{\lceil \frac{r_0}{r_{n-1}} \rceil \beta_{n-1} r_{n-1} p^{PLT}} \frac{d_0^2 + \sum_{i=1}^{n-1} (d_i^2 - d_{i-1}^2)}{d_{n-1}^2} < 1$ because $\beta_0 < \beta_{n-1}$ [18-20] infers $\beta_0 r_0 < \beta_{n-1} r_0$ and $p^{DF} = p^{PLT}$ (both p^{DF} and p^{PLT} are the transmission probability of the multicasting node via the channel with rate r_{n-1}); when $\beta_{n-1} r_{n-1} p^{PLT} < R < \beta_0 r_0 p^{DF}$, expression (1) can be simplified to $\frac{d_0^2 R + R \sum_{i=1}^{n-1} (d_i^2 - d_{i-1}^2)}{d_{n-1}^2 \lceil \frac{r_0}{r_{n-1}} \rceil \beta_{n-1} r_{n-1} p^{PLT}} < 1$ since $R < \beta_0 r_0 p^{DF}$ infers $R < \beta_{n-1} r_0 p^{PLT}$. Thus, the above three cases show

⁵The expression $\lceil \frac{r_0}{r_{n-1}} \rceil$ represents the smallest integer greater than $\frac{r_0}{r_{n-1}}$.

$\frac{T_D}{T_P} < 1$, i.e., the average throughput of PLT overtakes that of DF.

More specifically, the average throughput improvement of PLT is $\frac{T_P - T_D}{T_D} \geq \frac{\min\{R, \beta_{n-1} r_{n-1} p^{PLT}\} d_{n-1}^2 \lceil \frac{r_0}{r_{n-1}} \rceil}{d_0^2 \min\{R, \beta_0 r_0 p^{DF}\} + \sum_{i=1}^{n-1} (d_i^2 - d_{i-1}^2) \min\{R, \beta_i r_i p^{DF}\}} - 1$.
Q.E.D

IV. ALTERNATIVE RATE TRANSMISSION

Although PLT requires a simple process to effectively improve transmission ranges with high throughput, its significant benefit relies on the availability of orthogonal channels. With limited channel diversity in practice, we propose alternative rate transmission (ART). ART classifies WMN multicast nodes as *regular nodes* and *PLT nodes*. To limit usage of orthogonal channels (so that there are enough for PLT), regular nodes use single channels to transmit at the benchmark rate (R). PLT nodes employ PLT transmissions to multicast packets at the PLT rate (\tilde{R}). This section gives the method of ART (Theorem 2) to assign the two types of roles to nodes on a multi-hop multicast path so that high-performance coverage can be greatly extended with the minimum number of orthogonal channels. Then, the values of R and \tilde{R} that benefit the best balance between coverage and performance over multiple hops are discussed.

A. Alternative Rate Transmission

As analyzed in Fig. 1, WMN multicasting experiences complicated interference (caused by consecutive transmissions and parallel delivery) which negatively affects performance-guaranteed wireless multicasting coverage. ART controls interference caused by consecutive transmissions with the minimum number of orthogonal channels by assigning regular and PLT roles to multicasting nodes in the way defined in Theorem 2.

Theorem 2 For any path in a WMN multi-hop multicast system, in order to use the minimum number of orthogonal channels to make the most of the high-throughput coverage advantage provided by PLT, ART should assign nodes at the $j(\lceil \frac{\tilde{\mu}}{d} \rceil + 1)$ th hops ($j \in N$) as PLT nodes and nodes at all other hops as regular nodes, where d and $\tilde{\mu}$ are the radiuses of the transmission range and the interference range of transmission rates R and \tilde{R} respectively.

Proof. When ART employs \tilde{R} at the $j(\lceil \frac{\tilde{\mu}}{d} \rceil + 1)$ th hops, there are $\lceil \frac{\tilde{\mu}}{d} \rceil$ hops of regular transmissions with rate R between two closest PLT nodes. To avoid the interference between these regular nodes, the number of required orthogonal channels is $\min\{\lceil \frac{\tilde{\mu}}{d} \rceil, 3\}$. The reason for introducing 3 into the expression is because neighboring or hidden-terminal interference on a multi-hop path can be avoided if any 3 consecutive hops on the path use orthogonal channels. Then, adding the $\lceil \frac{R}{\tilde{R}} \rceil$ channels required by a PLT node⁶, the total number of channels required by an ART transmission is $(\lceil \frac{R}{\tilde{R}} \rceil + \min\{\lceil \frac{\tilde{\mu}}{d} \rceil, 3\})$.

⁶The two closest PLT nodes do not interfere with each other as they are not in each other's interference coverage.

For a non-ART transmission, assume that there are m regular nodes between the two closest PLT nodes. To avoid interference between m regular nodes, the number of required orthogonal channels is $\min\{m, 3\}$.

- When $m > \lceil \frac{\check{\mu}}{d} \rceil$, we have $m \geq 3$ because $\check{\mu} > d$ implies $\lceil \frac{\check{\mu}}{d} \rceil \geq 2$. If $m = 3$, the ART transmission is actually employed. If $m > 3$, the non-ART transmission underuses PLT transmissions and hence cannot achieve the best coverage performance. Furthermore, the number of orthogonal channels remaining to address external interference by this non-ART transmission should be equal to that unused by the ART transmission. This is because both the ART transmission and the non-ART transmission with $m > 3$ require three orthogonal channels to avoid interference between consecutive regular hops.
- When $m < \lceil \frac{\check{\mu}}{d} \rceil$, $3\lceil \frac{R}{\check{R}} \rceil$ channels are required to avoid interference between PLT nodes on the path. Adding the $\min\{m, 3\}$ orthogonal channels used by regular nodes to remove interference caused by consecutive transmissions, a total number of $3\lceil \frac{R}{\check{R}} \rceil + \min\{m, 3\}$ orthogonal channels are required. We have

$$[3\lceil \frac{R}{\check{R}} \rceil + \min\{m, 3\}] - [\lceil \frac{R}{\check{R}} \rceil + \min\{\lceil \frac{\check{\mu}}{d} \rceil, 3\}] > 0.^7 \quad (2)$$

That is, this non-ART transmission needs more orthogonal channels to avoid interference caused by consecutive transmissions than the ART transmission. Accordingly, it also means that fewer orthogonal channels remain to avoid potential external interference by nodes not on this non-ART transmission path.

Altogether, the use of \check{R} at the $j(\lceil \frac{\check{\mu}}{d} \rceil + 1)$ th hops is more efficient in controlling the usage of orthogonal channels while improving the high-throughput transmission coverage. Q.E.D

We use an example in Fig. 4 to illustrate the node role assignment of ART. Suppose $\frac{R}{\check{R}} = 1.6$ and $\frac{\check{\mu}}{d} = 1.8$. Nodes at the $j(\lceil \frac{\check{\mu}}{d} \rceil + 1)$ th hops are nodes 2 and 5. ART assigns them to be PLT nodes. These PLT nodes employ $\lceil \frac{R}{\check{R}} \rceil = 2$ channels in parallel to transmit at \check{R} . All other nodes 0, 1, 3, and 4 are regular nodes that transmit at R .

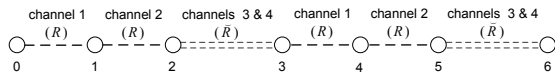


Fig. 4. An example of the alternate rate transmission in a line topology.

The ART transmission in Fig. 4 is interference-free if 4 orthogonal channels are available. The effectiveness of ART in saving channels may be called into question because 4 orthogonal channels are needed to avoid interference, rather than 3 that would be necessary in such a line topology. However, in practice, wireless multicast networks are much more complicated than a line topology. For the transmission in Fig. 5, node 0 is the sender and nodes 1 ~ 6 are receivers.

⁷ Note that $m < \lceil \frac{\check{\mu}}{d} \rceil$. Then, if $\lceil \frac{\check{\mu}}{d} \rceil < 3$, expression (2) can be simplified as $2\lceil \frac{R}{\check{R}} \rceil + m - \lceil \frac{\check{\mu}}{d} \rceil$. Since both m and $\lceil \frac{\check{\mu}}{d} \rceil$ are less than 3, it infers that $m - \lceil \frac{\check{\mu}}{d} \rceil < -1$ and hence $2\lceil \frac{R}{\check{R}} \rceil + m - \lceil \frac{\check{\mu}}{d} \rceil > 0$. By the similar way, expression (3) can be proved for the cases $m < 3 < \lceil \frac{\check{\mu}}{d} \rceil$ and $m > 3$.

Fig. 5 (a) shows that 5 orthogonal channels are required for avoiding interference if only using the benchmark rate. In Fig. 5 (b), node 1 employs PLT that uses 2 low-rate channels to cover nodes 2 ~ 5. With ART, node 4 receives on channels 2 and 3 instead of channel 1 (Fig. 5 (a)). Also, node 5 may reuse channel 1 to transmit to node 6 without interfering other coexisting transmissions. ART saves 2 orthogonal channels in this example.

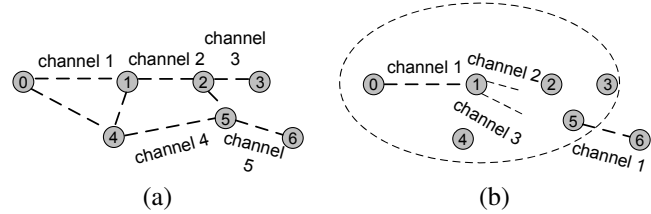


Fig. 5. An example of ART in a multicast communication.

B. Benchmark Rate and PLT Rate

Bearing the motivation of improving both performance and coverage in mind, by referring to our observations in [18] - wireless transmissions may achieve high throughput across wide areas by using multiple hops, ART regular transmissions should use such a rate (i.e., the benchmark rate R) so as to provide the best balance between coverage and performance over multiple hops. More specifically, the benchmark rate R helps to deliver multimedia data to the greatest coverage with guaranteed delays and throughput. We now analyze how to achieve R among n available rates.

For a multimedia flow with the burstiness $\sigma > 0$ and the average transmission rate $\rho > 0$, based on [13], the input traffic load meets $\int_t^{t+\tau} R(t)dt \leq \sigma + \rho\tau$, where $R(t)$ is the rate function of multimedia traffic. If the output with rate r_i can travel H_i hops (with guaranteed throughput) and the transmission probability at the j th ($j \in [0, H_i - 1]$) hop is $p_{i,j}$, the achievable output capacity at this hop is $r_i\beta_{i,j}p_{i,j}$, where $\beta_{i,j}$ is the throughput reduction factor of rate r_i at the j th hop. It infers that the one-way delay of the multicast flow

at this hop is $\frac{\sigma + \rho\tau}{r_i\beta_{i,j}p_{i,j}}$. Let $\frac{1}{\beta_i p_i} = \frac{\sum_{j=0}^{H_i-1} \frac{1}{\beta_{i,j} p_{i,j}}}{H_i}$. Then, the one-way delay for the multimedia flow to be transmitted on the H_i -hop path is $\sum_{j=0}^{H_i-1} \frac{\sigma + \rho\tau}{r_i\beta_{i,j}p_{i,j}} = \frac{H_i(\sigma + \rho\tau)}{r_i\beta_i p_i}$.

Hence, the greatest coverage for transmissions with rate r_i achieving guaranteed delays in delivery of complete multimedia data has an upper bound of

$$H_i d_i \leq \frac{d_i \bar{D} r_i \beta_i p_i}{\sigma + \rho\tau}, \quad (3)$$

where \bar{D} is the end-to-end delay bound and d_i is the radius of the transmission range of rate r_i . ART selects the rate that contributes the maximum value for expression (3) as the benchmark rate R .

For the PLT transmission rate, Theorem 3 presents equations for achieving \check{R} in order to gain the best performance-guaranteed coverage under the constraint of available orthogonal channels.

Theorem 3 In order to achieve the best channel utilization to gain the largest throughput-guaranteed transmission coverage, the rate r_i satisfying the following expression should be the PLT rate \tilde{R}

$$\max\left\{\frac{\lceil\frac{\mu_i}{d}\rceil \times d + d_i}{\min\{3, \lceil\frac{\mu_i}{d}\rceil\} + \lceil\frac{R}{r_i}\rceil + \psi}, i \in [0, n-1]\right\},$$

where $\psi = \lceil\lambda\mu_i\rceil + (\lceil\lambda\mu\rceil - 3)\lceil\frac{\mu_i}{d}\rceil + 1$, μ_i and μ are the radiuses of interference ranges of rates r_i and R (the benchmark rate of regular nodes) respectively, d is the radius of transmission range of rate R , and λ is the average node distribution density on a transmission path in the system.

Proof. Since a transmission coverage is proportional to the square of its radius, a bigger radius implies a bigger transmission coverage. Therefore, we employ the ratio between the largest throughput-guaranteed radius to the number of required orthogonal channels as the metric to choose the PLT rate \tilde{R} . Suppose PLT employs the i th available rate, i.e., r_i . Based on the proof of Theorem 2, to avoid interference caused by consecutive transmissions, the number of orthogonal channels required by ART is $\min\{3, \lceil\frac{\mu_i}{d}\rceil\} + \lceil\frac{R}{r_i}\rceil$.

Denote the average node distribution density on a transmission path as λ . To avoid interference caused by parallel delivery, we calculate the number of orthogonal channels required between two PLT nodes because these channels can be reused by nodes between other pairs of PLT nodes. A PLT node has maximally $(\lceil\lambda\mu_i\rceil - \lceil\frac{\mu_i}{d}\rceil)$ neighboring nodes that are not on the path; the next-hop regular node of the PLT node has maximally $(\lceil\lambda\mu\rceil - 1)$ neighboring nodes that are not on the path; each of the other $(\lceil\frac{\mu_i}{d}\rceil - 1)$ regular nodes between two PLT nodes covers 2 nodes on the path and hence needs maximally a set of $(\lceil\lambda\mu\rceil - 2)$ orthogonal channels to avoid external interference. Therefore, a total number of $\psi = \lceil\lambda\mu_i\rceil + (\lceil\lambda\mu\rceil - 3)\lceil\frac{\mu_i}{d}\rceil + 1$ orthogonal channels is maximally needed to remove interference from nodes that do not belong to the path.

For the transmission distance of ART, it is not hard to obtain $\lceil\frac{\mu_i}{d}\rceil \times d + d_i$. Then, the per channel transmission distance achieved by ART that uses R or r_i is $\frac{\lceil\frac{\mu_i}{d}\rceil \times d + d_i}{\min\{3, \lceil\frac{\mu_i}{d}\rceil\} + \lceil\frac{R}{r_i}\rceil + \psi}$, $i \in [0, n-1]$. Hence, to achieve the best channel utilization in terms of increasing transmission coverage, the radius of the transmission range of PLT transmissions should meet

$$\max\left\{\frac{\lceil\frac{\mu_i}{d}\rceil \times d + d_i}{\min\{3, \lceil\frac{\mu_i}{d}\rceil\} + \lceil\frac{R}{r_i}\rceil + \psi}, i \in [0, n-1]\right\}.$$

Q.E.D

V. LINK-CONTROLLED MULTI-RATE MULTI-CHANNEL MULTICASTING TREE (LC-MRMC)

This section designs the *link-controlled multi-rate multi-channel multicast* (LC-MRMC) algorithm to extend performance-guaranteed multicast coverage by using ART and controlling interference analyzed in Fig. 1. Unlike our study on single-group multicast [18], this paper focuses on multi-group multicasting communications, a more general case in practical systems.

A. The LC-MRMC Weight

With our ART-based multicast [18], each group needs to run an individual multicast tree. Then, in a WMN with multiple multicast groups, a node (e.g., a forwarding WMN router) may play different roles (i.e., PLT or regular) in different groups, causing complicated multicasting communications as well as increased interference. Hence, new developments are required to support multi-group MRMC multicast. We propose to develop multicast in the backbone of a WMN system that can be shared by different multicasting groups. More specifically, the new LC-MRMC algorithm constructs a multicast tree rooted at multiple mesh gateways (MGs), allowing multicast senders to load data to the multicast tree via their closest MGs and hence benefitting real-time multicast communications. The following metrics are employed to construct the LC-MRMC tree for multi-group multicasting.

a. *ART hop distance* is the number of hops on an ART path (i.e., a path built up by referring to Theorems 2 & 3). A path with shorter ART hop distance is preferred because of shorter delays and less transmission contention.

b. *Nodes with rich and eligible connectivity*. Eligible connectivity refers to connections to multicast nodes which do not have forwarders (called uncovered nodes) as opposed to those having forwarders (called covered nodes). A WMN node that has more eligible connections is preferred for the role of forwarding node. This metric helps to reduce the number of forwarders and hence limits interference/conflict caused by parallel multicast transmissions.

c. *Reliability*. A reliable path has priority to be a multicast path because wireless links may be lost frequently affecting the continuity of multimedia presentation.

To combine the above metrics, we propose the LC-MRMC weight ω . For path i connecting a MG to at least one receiver, its LC-MRMC weight is defined as

$$\omega_i = \frac{1}{h_i^{ART}} \times \sum_{j=1}^{h_i^{ART}} \frac{D_{i,j}}{N_{i,j}} \times \prod_{j=1}^{h_i^{ART}} (1 - l_{i,j}), \quad (4)$$

where h_i^{ART} is the ART hop distance to the closest root/MG on path i , $D_{i,j}$ is the total number of child nodes at the j th hop that haven't found their forwarders, $N_{i,j}$ is the total number of neighboring nodes at the j th hop, and $l_{i,j}$ is the loss rate at the j th hop. In this expression, $\frac{D_{i,j}}{N_{i,j}}$ is the metric for evaluating whether a mesh node covers more child nodes that haven't found forwarders or not (i.e., rich eligible connectivity), and $\prod_{j=1}^{h_i^{ART}} (1 - l_{i,j})$ is the metric for evaluating path reliability. A path with a larger LC-MRMC weight has the priority to become a multicast path.

B. The LC-MRMC Algorithm

We assume the existence of a group manager (GM)⁸ in our multicast system. The GM of LC-MRMC maintains information about group senders/receivers and system topology, as well as implementing ART analysis based on Theorems 2

⁸In the literature, studies have provided solutions for the development of a GM, such as the RRAS multicast group manager.

& 3. Multicast senders and receivers contact the GM to get information regarding the group ID, the benchmark rate, and the PLT rate. Note that, for the sake of reliable multicast, it may be necessary for multiple GMs to coexist.

The construction of an LC-MRMC tree is triggered by the registration procedure of receivers of multicast groups. In detail, a receiver broadcasts to its multicast sender(s) a REGISTRATION packet which mainly includes the fields of Group_ID (identifying the multicast group(s) that the receiver belongs to), Hop_Count (the number of hops from a mesh node to its closest root/MG), and Forwarders_List (recording the IP address, node type⁹, and link loss rate of a mesh node that forwards this REGISTRATION message). Hop_Count is initially set to 0 by a receiver but increases by 1 at each intermediate node forwarding this REGISTRATION. Each node also updates the Forwarder_List by recording its IP address, node type, and link loss rate (required by equation (4)) in this field. The REGISTRATION message is broadcasted at the benchmark rate R and each node only broadcasts the same REGISTRATION message once. In this way, while unnecessary broadcasting traffic is avoided, the REGISTRATION message is also able to carry information about mesh gateways (MGs) that are close to the paths connecting the receiver to its sender(s).

The GM of LC-MRMC assigns the sender of the multicast group with the lowest Group_ID as the LC-MRMC coordinator. Each sender encapsulates MG information (collected by REGISTRATIONS) in a GATEWAY packet and unicasts this packet to the LC-MRMC coordinator. The LC-MRMC coordinator then sorts all MGs (reported by REGISTRATIONS) in decreasing order of "receiver number", calculated as follows. The first MG is the one receiving REGISTRATIONS from the greatest number of receivers, the second MG is that which received the most REGISTRATIONS from receivers not already accounted for by the first, the third has the most new receivers not accounted for by the first and second, and so on. This continues until the set of MGs accounts for all receivers - i.e. there is within the group an MG recipient for a REGISTRATION from every receiver. The roots of the constructed LC-MRMC tree consist of this set. This benefits the fast construction of an LC-MRMC tree as the minimum number of roots carry out the following procedures.

An LC-MRMC root broadcasts an ACK message to the receiver(s) from which this root receives a REGISTRATION, with the rate \tilde{R} at the $j(\lceil \frac{H}{d} \rceil + 1)$ th hops ($j \in N$) and the rate R at all other hops. This is to support the creation of ART paths. The ACK packet records the IP address and the ART hop distance (to the root) of each forwarder. On receiving an ACK packet, a receiver encapsulates the IP addresses and the ART hop distances (from the ACK packet) in a TOPOLOGY packet and unicasts this packet back to the root. Each root sends its received TOPOLOGY packet to the LC-MRMC coordinator which then assigns all mesh nodes included in TOPOLOGY packets a level number. The level number of a mesh node refers to the shortest ART hop distance among

⁹Node type is set to identify whether a node is a mesh gateway or a mesh router.

all the paths connecting this node to its closest MG/root. To select the LC-MRMC on-tree members, following steps 8 - 11 in Algorithm 1, starting from the second highest level, the LC-MRMC coordinator selects LC-MRMC forwarders based on their values for $\frac{D}{N} \times (1 - l)$, where D and N are the total number of uncovered child nodes and neighboring nodes of a node respectively, and l is the link loss rate of this node. When all selected forwarders at the second highest level can cover all receivers at the highest level, the LC-MRMC coordinator continues to select new forwarders at the third highest level in the same manner. The procedure continues until the on-tree forwarders at the second level are selected. On each multicast path, following steps 12 - 17, the LC-MRMC coordinator assigns channels to regular nodes and PLT nodes to complete the construction of the LC-MRMC tree. Note that if there is a low availability of orthogonal channels, channels with low overlap will be used by the algorithm. Finally, to quickly and reliably load data to the LC-MRMC tree for the multicast of these data to receivers, each sender employs the weighted gateway uploading algorithm [22] to select the MG having the best balance between reliable throughput and short delays as its uploading gateway. An uploading gateway communicates with LC-MRMC roots via Internet links by the same way that we presented in [22]. The selection of uploading gateways runs in parallel with the receivers' registration procedure.

Algorithm 1 The Link-Controlled Multi-rate Multi-channel Multicasting Tree

Input: Multicast senders and multicast receivers;
 Output: The constructed LC-MRMC tree;

-
1. A receiver broadcasts a REGISTRATION packet (with Hop_Count set as 0) to its multicast sender(s); a multicast sender searches its uploading MG by the weighted gateway uploading algorithm [22];
 2. An intermediate node forwards a REGISTRATION from the same receiver once, after updating Hop_Count and Forwarder_List;
 3. The sender with the lowest Group_ID becomes the LC-MRMC coordinator;
 4. Each sender unicasts a GATEWAY packet (with MG information) to the coordinator; the coordinator selects the minimum number of MGs as LC-MRMC roots by sorting all involved MGs in decreasing order of "receiver number";
 5. An LC-MRMC root broadcasts an ACK message to the receivers from whom it receives a REGISTRATION via ART transmissions;
 6. Based on the received ACK message, a receiver replies a TOPOLOGY packet to inform its root of the IP addresses and the ART hop distances of nodes on the way;
 7. All roots send their received TOPOLOGYs to the coordinator; the coordinator assigns nodes involved in exchanging the above packets into different levels, and sets $j = H - 1$;
// H is the maximum number of ART hops between roots to all receivers
 8. **While** $j > 0$
 9. Among all non-forwarding nodes at level j , the coordinator selects the one with the largest $\frac{D}{N} \times (1 - l)$ as an

LC-MRMC forwarder;

10. **If** forwarders at level j covers all LC-MRMC forwarders/receivers at level $(j + 1)$, $j = j - 1$;

11. **Otherwise**, goes to step 9 to continue selecting on-tree forwarders at level j ;

12. The coordinator arranges orthogonal or low-overlapping channels into a channel set with orthogonal ones listed ahead of low-overlapping ones, and sets $j = 0$;

13. **While** $j < (H - 2)$

14. **If** forwarders at level j are regular forwarders,

15. The coordinator assigns the c th channel in the channel set to forwarders at level j ; // c is the remainder of the expression $(j \div L)$, where L is the total number of channels in the channel set

16. **Otherwise**, // level- j forwarders are PLT forwarders

17. The coordinator assigns the c th channel to the $(c + \lceil \frac{R}{R} \rceil)$ th channel to forwarders at level j ;

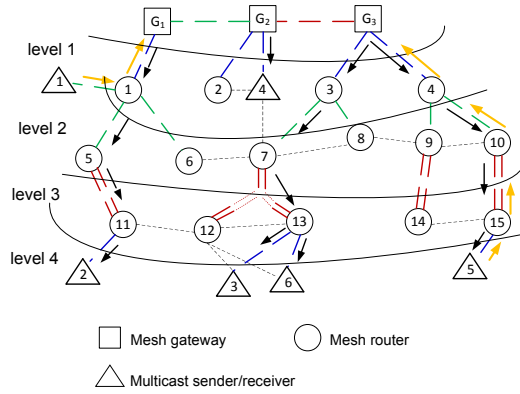


Fig. 6. An example of the LC-MRMC multicast.

To illustrate Algorithm 1, in Fig. 6, we use triangle nodes to represent multicast senders and receivers among which nodes 1 & 5 are multicast senders. Based on [22], we assume that G_1 and G_3 are the uploading gateways of nodes 1 and 5. Suppose node 1 is the LC-MRMC coordinator. Node 5 encapsulates the MGs that have forwarded its receivers' REGISTRATIONS into a GATEWAY packet and unicasts the packet to the coordinator via G_3 and Internet links. The coordinator sorts all MGs in decreasing order of "receiver number": G_3 , G_1 , and G_2 . The three MGs become LC-MRMC roots as each of them is required by at least one receiver to receive REGISTRATION packets. Then based on the ART hop distance, the coordinator arranges all nodes involved in forwarding REGISTRATIONS into different levels. That is, as shown in the figure, starting from level 3 (i.e., the second highest level), the coordinator selects LC-MRMC forwarders that can reliably cover the greatest number of uncovered group receivers at level 4. Suppose mesh routers 11 ~ 15 have the same loss rates. As mesh routers 12 and 13 connect to the same two receivers, i.e., $D_{12} = D_{13} = 2$, to select a forwarder between them, the values of N_{12} and N_{13} are compared: $N_{12} = 4$ and $N_{13} = 3$. Critically, mesh router 12 is neighbouring mesh router 11 which is the only node providing a connection to the

receiving node 2. Hence, after mesh router 11, mesh router 13 becomes the second forwarder at level 3. Then the only mesh router (i.e., mesh router 15) that connects to the remaining receiving node 5 becomes the forwarder at level 3. Hereafter, the coordinator selects forwarders at levels 2 and 1 by just as it does to select level-3 forwarders. In Fig. 6, the constructed LC-MRMC tree is illustrated by the black arrows and the ART channel assignment on the LC-MRMC tree is shown by the colored dotted lines. The orange arrow lines demonstrate that multicast senders upload data to their uploading gateways which then distribute the data to other roots via Internet links (as we studied in [22]) as well as to receivers via the LC-MRMC tree.

VI. SIMULATION EVALUATION

In this section, we use the discrete event network simulator NS2.33 to conduct an extensive simulation-based evaluation for ART and LC-MRMC. Table I lists the simulation parameters. The video transmission rate range in the table is generated by varying the frame rates of the MPEG-4 file *StarWarsIV.dat*. Performance curves in the figures of this section are plotted based on the average value of 20 simulation runs. The simu-

TABLE I
SIMULATION PARAMETERS

Parameter	Value
Simulator	NS2.33
Frequency	2.4GHz
Propagation Model	Nakagami
MAC Protocol	802.11
Transmission Power	15dBm
Receive Threshold of 1.0 Mbps Transmissions	-94dBm
Receive Threshold of 2.0 Mbps Transmissions	-91dBm
Receive Threshold of 5.5 Mbps Transmissions	-87dBm
Receive Threshold of 11 Mbps Transmissions	-82dBm
Packet Type	RTP/UDP
Packet Size	1400 bytes
NS-2 Video Trace File	StarWarsIV.dat
Video Frame Rate	25 frames/second
Video Size	89998 (I/P/B) frames
Video Flow Transmission Rates	[90Kbps, 2Mbps]
Simulation Duration	500ms
Number of Orthogonal Channels	4
Delay Bound	150ms

lations mainly observe the following performance metrics.

- Average throughput ratio (ATR). The average throughput is defined as $AT = \frac{\sum_{i=1}^n T_i}{n}$, where n is the number of receivers and T_i is receiver i 's throughput. The average throughput ratio is expressed by $ATR = \frac{AT}{C}$, where C represents the total amount of traffic load that needs to be transmitted per second. ATRs demonstrate how well a network transmission scheme can deliver high quality multimedia flows to users. A larger ATR is better.
- Average delays (AD) are defined as $AD = \frac{\sum_{i=1}^n d_i}{n}$, where d_i is the average delay of all packets received by receiver i . Delays exceeding the bound cause lag which adversely affects the ability of users to communicate in real time.
- Average multicast peak signal-to-noise ratio (AMPSNR) is calculated by $AMPSNR = \frac{\sum_{i=1}^n APNSNR_i}{n}$, where

$AMPSNR_i$ is the average PSNR of video traffic at the i th receiver. PSNR is a metric that captures the performance error between the original and the reconstructed video frames. AMPSNR helps to assess the application-level QoS of video multicasting transmissions. In our simulations, PSNR data are collected by using the EvalVid tool-set [24].

- The longest multicast distance (LMD) refers to the physical distance between the sender and its farthest receiver(s). LMD is employed to evaluate the potential multicast coverage that can be achieved by a network transmission scheme. An extended performance-guaranteed wireless coverage is a major goal of this paper.

A. ART Evaluation

The first group of simulations looks into the ART generated by Theorems 2 & 3 - whether ART provides the best balance between throughput and coverage among all channel and rate allocation plans. Our simulations employ the mesh topology in Fig. 7 (a). The blue dotted lines in the topology illustrate the 10-hop path that we will use to evaluate ART transmissions.

TABLE II
 COMPARISON OF EFFECTIVE THROUGHPUT AND COVERAGE RADIIUSES OF DIFFERENT TRANSMISSION RATES

Transmission Rate	Effective Throughput	Transmission Range Radiuses	Interference Range Radiuses
11Mbps	4.77Mbps	283m	425m
5.5Mbps	3.22Mbps	351m	526m
2Mbps	1.5Mbps	369m	544m
1Mbps	0.85Mbps	482m	723m

We first simulate one-hop transmissions (using the first hop on the 10-hop path) with the four different rates (11Mbps, 5.5Mbps, 2Mbps, and 1Mbps) and demonstrate the results in Table II. We then examine Theorem 2 by applying PLT transmissions at different hops to observe the achievable throughput ratios. The benchmark rate is 11Mbps and the PLT rate is 5.5Mbps. Based on Theorem 2, ART should implement PLT transmissions at every 3rd hop. Fig. 7 (b) plots average throughput ratio curves when PLT is used at every 2nd hop, every 3rd hop, or at random hops. The results show that the two non-ART schemes (i.e., PLT at every 2nd hop or at random hops) achieve similar throughput performance - much lower than that achieved by ART. This is because interference in ART is greatly controlled when applying PLT transmissions at appropriate hops. Hence, the simulation results prove the efficiency of Theorem 2 in improving throughput under the limitation of orthogonal channels. In order to examine Theorem 3, we evaluate transmissions that follow the ART pattern of allocating regular and PLT nodes (i.e., Theorem 2) but employ different transmission rates at PLT nodes. Three pairs of benchmark rates and PLT rates are compared: (11Mbps, 5.5Mbps), (11Mbps, 2Mbps), and (11Mbps, 1Mbps). The 11Mbps benchmark rate is decided based on (2). More specifically, according to (2), when transmitting the same video flows, the benchmark rate should have the maximum value for $d_i r_i \beta_i$, where d_i is the radius of rate

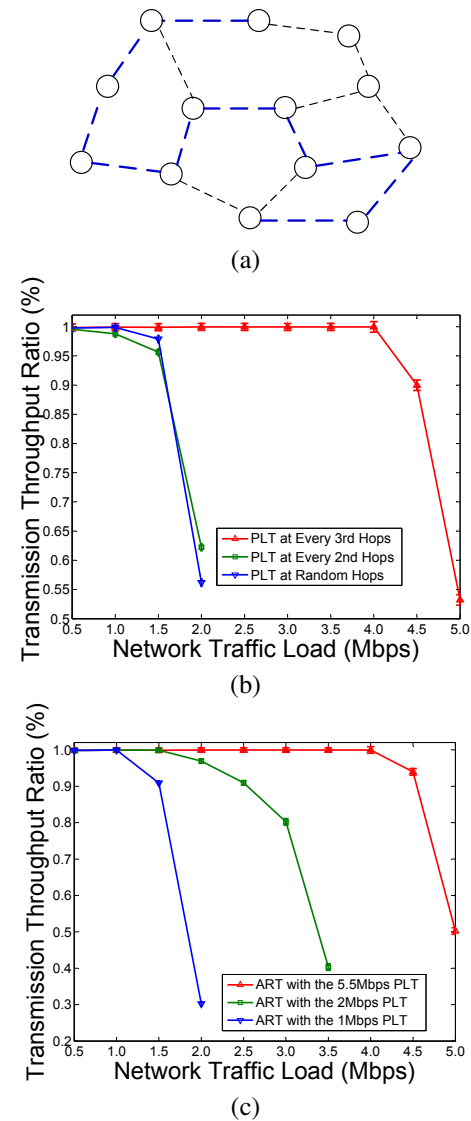


Fig. 7. Simulation topology of ART evaluation (a). Comparison of throughput ratios achieved on the 10-hop path when (b) the PLT adopted at different hops, and (c) the PLT with different transmission rates.

r_i 's transmission range and $r_i \beta_i$ is the effective throughput of rate r_i . By combining the transmission range radius with the effective throughput of each transmission rate, the 11Mbps rate is used as the benchmark rate. Fig. 7 (c) gives the throughput ratios achieved by different rate pairs. The rate pair (11Mbps, 5.5Mbps) achieves the best throughput performance. If we input the parameters of rate pairs (11Mbps, 5.5Mbps), (11Mbps, 2Mbps), and (11Mbps, 1Mbps) in the expression $\frac{\lceil \frac{\mu_i}{d} \rceil \times d + \mu_i}{\min\{3, \lceil \frac{\mu_i}{d} \rceil\} + \lceil \frac{R}{r_i} \rceil + \psi}$ (Theorem 3), we get the values 156.0, 115.9, and 104.8 for the above rate pairs respectively. This shows that the simulation results match our theoretical analysis - the rate having the maximum value for $\frac{\lceil \frac{\mu_i}{d} \rceil \times d + \mu_i}{\min\{3, \lceil \frac{\mu_i}{d} \rceil\} + \lceil \frac{R}{r_i} \rceil + \psi}$ should be used by PLT transmissions.

The throughput-guaranteed transmission distance achieved by the above different transmission schemes when they carry 2Mbps traffic is 3034m for ART, 917m for PTL at every 2nd hops, 634m for PLT at random hops, 283m for ART

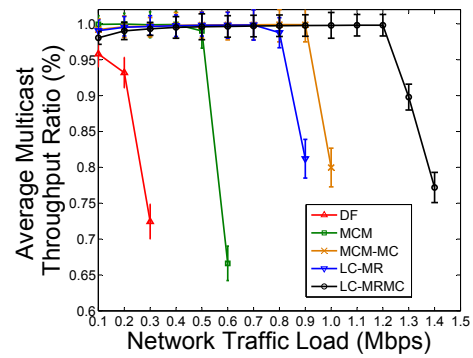
with 2Mbps PLT, and 283m for ART with 1Mbps PLT. By throughput-guaranteed transmission distance, we accumulate the physical distance of all hops that can achieve acceptable throughput from the sender. The limited number of orthogonal channels (4 channels) greatly affects the transmission distance of ART schemes using a PLT rate different from the one determined by Theorem 3. Particularly, for the ART with 2Mbps PLT and the ART with 1Mbps PLT, the lack of orthogonal channels causes the PLT transmissions of both schemes interfere with each other and hence degrades throughput quickly.

B. Performance Evaluation in a Random WMN

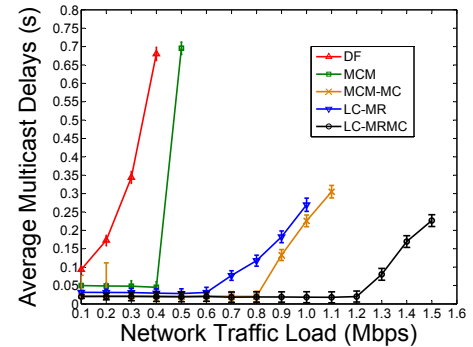
For evaluating LC-MRMC, we compare the average multicast throughput, the average multicast delay and the multicast coverage of the following five different wireless multicast schemes in a wireless network with 100 mesh nodes: DF [11], MCM which uses Breadth First Search to find the minimum number of relay nodes [16], MCM-MC which is a MCM tree with channel allocation [16], LC-MR which is our multicast tree without channel allocation, and our LC-MRMC. The locations (i.e., coordinates) of mesh nodes are randomly set by the simulations so as to achieve a distribution density such that there is on average 3.82 nodes within the range of 11Mbps transmissions. Among the 100 mesh nodes, 15 nodes are selected as group receivers. All other simulation settings are the same as the ones used for previous simulations.

Fig. 8 (a) shows the average multicast throughput ratios achieved by different multicast schemes. DF generates the worst throughput performance because its wireless multicast architecture uses resources inefficiently by transmitting the same multimedia traffic more than one time. Also, when using different transmission rates, nodes generate different transmission coverage causing complicated interference topology. For MCM and LC-MR that do not employ multiple channels, LC-MR achieves a higher average multicast throughput because it avoids more interference and employs more stable wireless nodes to multicast. MCM-MC and LC-MRMC are the multi-channel versions of MCM and LC-MR respectively. The reason for LC-MRMC to be able to carry a larger multicast traffic load (around 35% improvement) than MCM-MC does is because LC-MRMC uses PLT at appropriate hops to increase the coverage which not only results in the reduced number of multicast forwarders but also increases the distances between some hops.

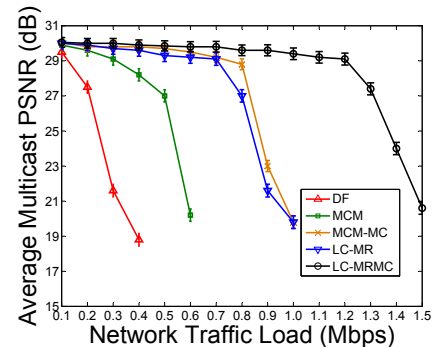
Fig. 8 (b) presents the average multicast delays. Each delay is the average value of the average delays of all receivers in the three groups. DF generates the longest delay even when the traffic load is low because interference causes longer queueing delays. LC-MR achieves better delay performance than MCM. One of the reasons is because PLT transmissions in LC-MR connect some nodes with only one hop which would be connected by multiple hops in MCM. For the comparison between LC-MR and MCM-MC, the employment of a shared multicasting backbone in LC-MR greatly controls interference and hence benefits the timely transmissions of multimedia traffic. Combining both throughput and delay performance,



(a)



(b)



(c)

Fig. 8. Comparison of the average throughput ratios (a), the average delays (b), and the average PSNR (c) achieved in the random WMN.

LC-MRMC can admit at least 38.9% extra video traffic with guaranteed delays and throughput as compared to other multicast schemes.

Fig. 8 (c) shows the average multicast PSNR performance of the five schemes. DF generates the worst average multicast PSNR performance. This is mainly because a DF node incurs different interfering ranges using different transmission rates, causing complicated interference which is difficult to control with a limited number of orthogonal channels. LC-MRMC achieves the best average multicast PSNR performance which can be explained by its formation of ART paths (limiting the number of wireless transmission hops and hence reducing the problem of signal fading), its construction of multicasting tree (decreasing the noise by interference-controlled multicast paths), and its employment of multiple channels (avoiding the weakening of signals by interference/contention). LC-

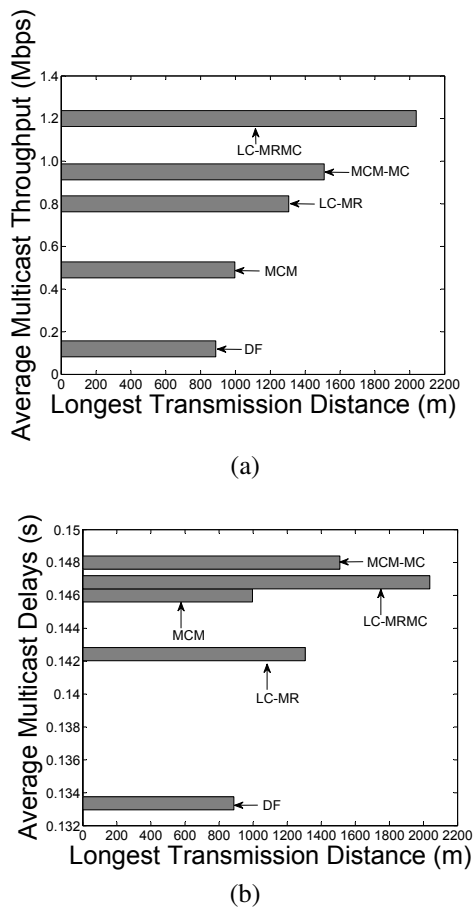


Fig. 9. Comparison of multicast coverage (a) with acceptable average multicast throughput and (b) with acceptable average multicast delays.

MRMC's average multicast PSNR performance is acceptable until network traffic load goes beyond 1.5Mbps.

We also evaluate the performance-guaranteed multicast coverage that can be achieved by these multicast schemes. Fig. 9 (a) shows the effective multicast throughput of the five schemes and the largest coverage within which their effective multicast throughput can be guaranteed. Fig. 9 (b) reports the maximum multicast coverage of different schemes when guaranteeing acceptable multicast delays. Via multiple hops, LC-MRMC can multicast 1.2Mbps video traffic to a greatest distance of 2035m with guaranteed delay performance 146.5ms. This shows that, in our simulations, LC-MRMC increases multicast coverage by more than 36% under higher traffic loads.

C. Performance Evaluation in Multi-group Multicasting

In this group of simulations, we observe the performance of the five multicast schemes in multi-group WMN multicasting. The WMN system is formed by 100 backbone nodes (i.e., mesh routers or mesh gateways) and 3 coexisting multicasting groups. Similar to the formation of the topology in the last section, the locations of the 100 backbone nodes are randomly set by the simulations so as to achieve a distribution density such that there are on average 3 nodes within the range of 11Mbps transmissions. For the 3 multicast groups, they are formed by mesh users who directly connect to the backbone

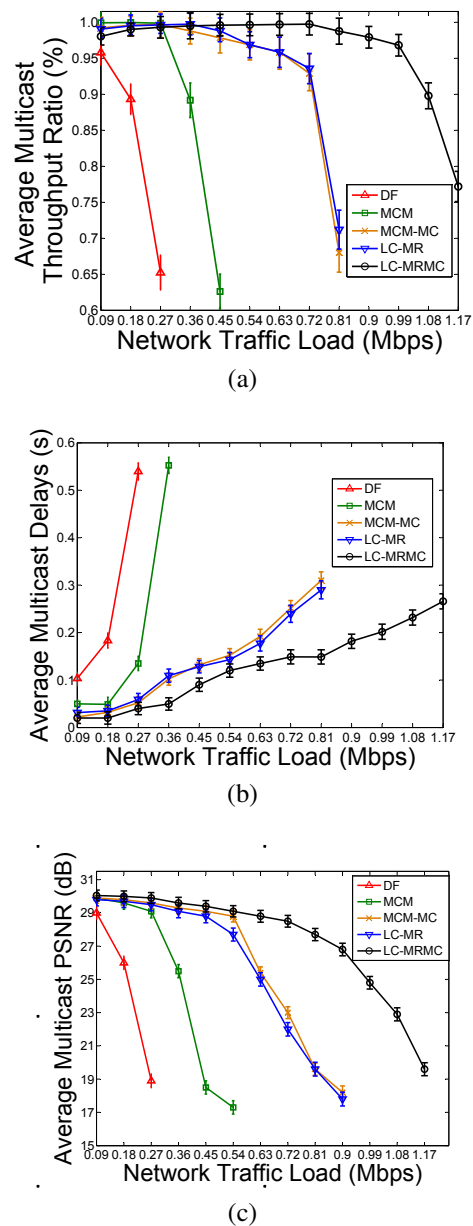


Fig. 10. Comparison of the average throughput ratios (a), the average delays (b), and the average PSNR (c) achieved in the multi-group multicasting WMN.

via a mesh router or a mesh gateways. Each group has 15 users. All other simulation settings are the same as those used for previous simulations.

Fig. 10 (a) shows the average throughput ratios, which demonstrates a comparison similar to that shown in Fig. 8 (a). DF generates the worst average throughput performance for the three multicasting groups. This is not only because of the transmission of the same traffic more than once but also caused by the complicated topology generated by different rates via different transmission directions. For MCM-MC, due to the limited number (i.e. four) of orthogonal channels used in the simulations, interference cannot be greatly controlled when there are three different groups of traffic requiring mesh nodes to play different roles in the topology. For LC-MR, a link-controlled multi-rate multicasting architecture is constructed to

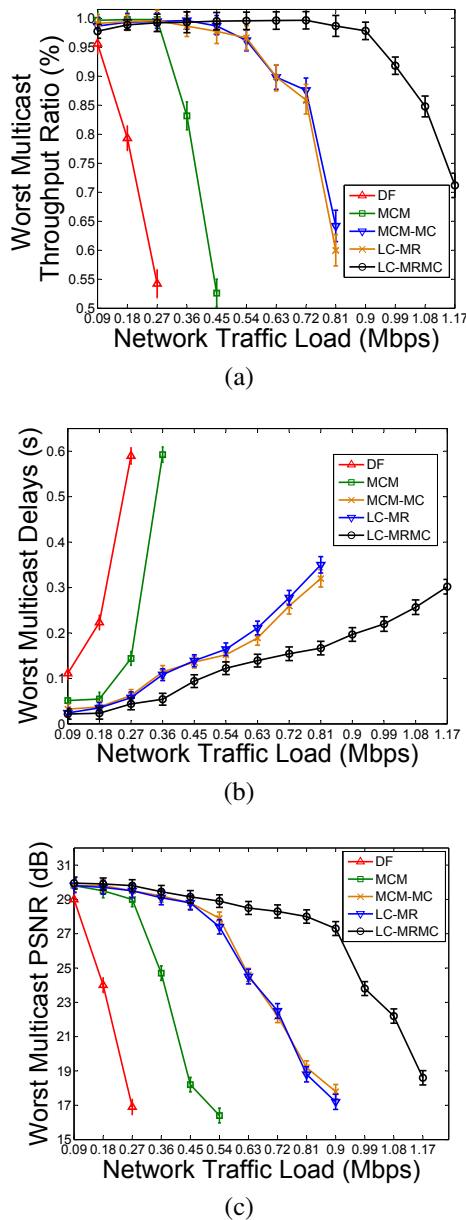


Fig. 11. Comparison of the worst throughput ratios (a), the worst delays (b), and the worst PSNR (c) achieved in the multi-group multicasting WMN.

be used by all the three multicasting groups as the backbone to distribute multimedia traffic avoiding complicated interference topologies. Hence, MCM-MC achieves a very slightly lower throughput performance than that of LC-MR in our simulations. LC-MRMC overtakes other multicasting schemes by employing a sharing multicasting tree for three transmission groups, employing PLT at appropriate hops and using multiple channels to avoid interference.

Fig. 10 (b) presents the average multicast delays. Each delay is the average value of the average delays of all receivers in the three groups. DF generates the longest delay even when the traffic load is low because interference causes longer queuing delays. LC-MR achieves better delay performance than MCM does. One of the reasons is because PLT transmissions in LC-MR connect some nodes by only one hop which would be

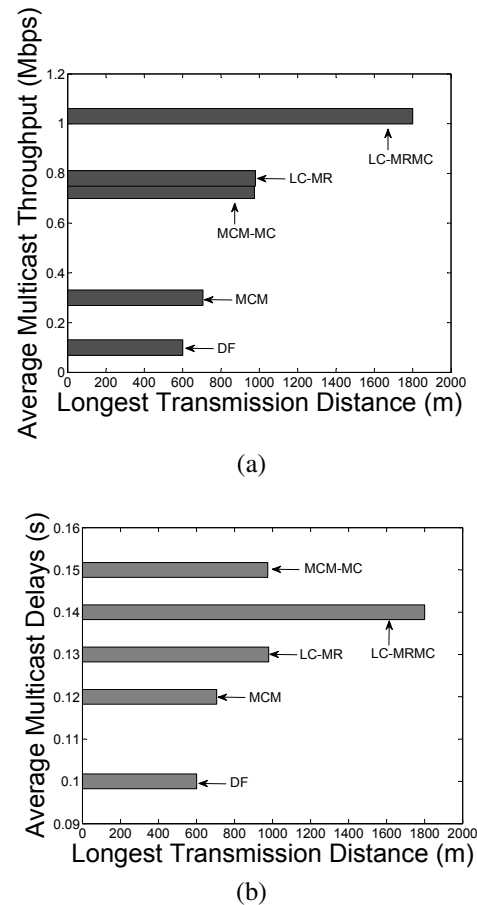


Fig. 12. Comparison of multicast coverage (a) with acceptable average multicast throughput and (b) with acceptable average multicast delays.

connected by multiple hops in MCM. For the comparison between LC-MR and MCM-MC, the employment of a shared multicasting backbone in LC-MR greatly controls interference and hence benefits the timely transmissions of multimedia traffic. Combining both throughput and delay performance, LC-MRMC can admit at least 38.9% extra video traffic with guaranteed delays and throughput as compared to other multicast schemes.

Fig. 10 (c) compares the average PSNR performance for the five schemes. As observed, LC-MRMC achieves the best average multicast PSNR performance owing to its multicast architecture shared by the three multicast groups. The plotted results in this figure can be explained much as the results in Fig. 8 (c).

Fig. 11 shows the worst throughput, delay, and PSNR performance among receivers in the three simulated groups. The difference between the worst multicast throughput ratio and the average multicast throughput ratio is 11% for DF carrying 270Kbps traffic, 10% for MCM carrying 450Kbps traffic, 7% for MCM-MC carrying 810Kbps traffic, 8% for LC-MR carrying 810Kbps traffic, and 5% for LC-MRMC carrying 1.17Mbps traffic. The difference between the worst multicast delay and the average multicast delay is 50ms for DF carrying 270Kbps traffic, 40ms for MCM carrying 450Kbps traffic, 30ms for MCM-MC carrying 810Kbps traffic, 40ms for

LC-MR carrying 810Kbps traffic, and 36ms for LC-MRMC carrying 1.17Mbps traffic. The difference between the worst multicast PSNR and the average multicast PSNR is 2dB for DF carrying 270Kbps traffic, 0.9dB for MCM carrying 540Kbps traffic, 0.8dB for MCM-MC and LC-MR carrying 810Kbps traffic, and 1dB for LC-MRMC carrying 1.17Mbps traffic. In short, the simulation shows that the performance (i.e., throughput, delays, and PSNR) variation between receivers in different groups is least when employing LC-MRMC multicasting, owing to the shared multicast architecture built to avoid link loss and save delays.

We then evaluate the longest transmission distance for each multicast scheme to achieve acceptable throughput and delays. The simulation attaches new nodes to the backbone multicast tree. Fig. 12 (a) shows the longest transmission distance associating with the supported multicast throughput of each multicast scheme. LC-MRMC spreads the video traffic across a much greater distance than other schemes do. This is mainly because the PLT transmissions of LC-MRMC enable certain hops to have longer distances with larger transmission capacity. Although LC-MR has the same multicast architecture as LC-MRMC does, the distance across which acceptable throughput can be achieved is shorter than in LC-MRMC due to the lack of channel diversity to avoid interference. Fig. 12 (b) presents the longest transmission distance without incurring unaccepted delays for each multicast scheme. LC-MRMC generates longer delays as it carries video traffic across much longer distances. Overall, in this group of simulations, LC-MRMC enables performance-guaranteed multicast to be carried to a wider area which is almost 80% greater than the distance reachable for other multicasting schemes.

Finally, Table III presents the control traffic load generated by the five schemes in order to establish their multicasting architectures. MCM-MC and MCM generate heavier control traffic loads than other schemes. This is because MCM-MC or MCM forwarders are selected randomly meaning that the shortest multicasting paths cannot be guaranteed (as with LC-MR and LC-MRMC) and thus more forwarders issue control packets to the network. Between MCM-MC and MCM, the channel arrangement of MCM-MC generates extra control packets. The control traffic load of DF is mainly caused by DF rate selection and DF channel allocation on multi-hop multicasting paths.

TABLE III
COMPARISON OF CONTROL TRAFFIC LOAD

DF	MCM	MCM-MC	LC-MR	LC-MRMC
138.81Kbps	159.21Kbps	169.97Kbps	76.03Kbps	81.67Kbps

VII. CONCLUSION

This paper showed how to exploit multiple channels and multiple transmission rates with simple procedures and light overheads to improve performance-guaranteed multicast transmission coverage. The transmission opportunity afforded by MRMC was investigated by proposing PLT. PLT enables a mesh node to employ multiple channels transmitting at a lower

rate (than the maximum available rate) in parallel to share the delivery of a full multimedia flow with an aggregated throughput across greater distances. We then designed ART which alternately uses regular transmissions and PLT transmissions to make the best of limited available channel and rate resources while promoting communication coverage with high throughput and short delay performance. ART became a key strategy in developing our LC-MRMC algorithm to multicast multimedia traffic across much larger areas wirelessly. LC-MRMC also controls multicast interference well and hence benefits high-throughput multicast. The results of our NS2 simulations proved that LC-MRMC distributes multiple groups of video flows to receivers with better performance across an area which is at least 80% larger than other existing MRMC schemes.

Although our proposed algorithms are evaluated based on IEEE 802.11b in the simulations, the algorithms and theoretical studies in this paper are developed without reliance on specific IEEE 802.11 MAC or physical settings. We consider interference incurred by the channel access control of IEEE 802.11 MAC, enabling our algorithms to be easily integrated with different IEEE 802.11 standards as long as WMN nodes are equipped with multiple radio interfaces (for attaching multiple channels). Furthermore, with the development of single NICs with multiple transceivers, our studies can be implemented without requiring nodes to have multiple interfaces. More recent standards such as IEEE 802.11ac offer more orthogonal channels (in multiple spectrum bands) which should benefit PLT or ART to perform better in balancing the tradeoff between communication quality and coverage. They also provide wider channel bandwidth, favourably supporting a LC-MRMC tree to be shared by multiple concurrent multimedia applications. Hence, we believe that our work in this paper will be well aligned with technology trends.

ACKNOWLEDGEMENT

This research is supported by the UK EPSRC grant EP/J017159/1.

REFERENCES

- [1] O. Karimi, J. Liu, and Z. Li. Multicast in Multi-channel Wireless Mesh Networks. In Proc. of IFIP Networking, pages 148-159, India, 2010.
- [2] S. Lim, Y. Ko, C. Kim, and N. Vaidya. Design and Implementation of Multicasting for Multi-Channel Multi-Interface Wireless Mesh Networks. (Springer) Wireless Networks 17:955972, 2011.
- [3] N. Lan, and N. Trang. Channel Assignment for Multicast in Multi-channel Multi-raido Wireless Mesh Networks. (Wiley) Wireless Communications and Mobile Computing, vol.9, pages 557-571, 2008.
- [4] S. Hon, K. Yeung, and K. Lui. Bandwidth-guaranteed Multicast in Multi-channel Multi-interface Wireless Mesh Networks. In Proc. of IEEE ICC, pages 1-5, Germany, 2009.
- [5] J. Choi, J. Na, K. Park, and C. Kim. Adaptive Optimization of Rate Adaptation Algorithms in Multi-Rate WLANS. In Proc. of IEEE ICNP, pages 144-153, China, 2007.
- [6] H. Zhu and G. Cao. rDCF: A Relay-Enabled Medium Access Control Protocol for Wireless Ad Hoc Networks. In IEEE Transactions on Mobile Computing, vol.5, issue 9, pages 1201-1214, 2006.
- [7] T. Kim, G. Jakllari, S. Krishnamurthy, and M. Faloutsos. A Unified Metric for Routing and Rate Adaptation in Multi-rate Wireless Mesh Networks. In Proc. of IEEE MASS, pages 242-251, Spain, 2011.
- [8] A. Kakhbod, and D. Teneketzis. An Efficient Game Form for Multi-Rate Multicast Service Provisioning. IEEE Journals on Selected Areas in Communications, vol.30, issue 11, pages 2093-2104, 2012.

- [9] O. Alay, T. Korakis, Y. Wang, and S. Panwar. Dynamic Rate and FEC Adaptation for Video Multicast in Multi-rate Wireless Networks. (ACM) Journal of Mobile Networks and Applications, vol.15, issue 3, pages 425-434, 2010.
- [10] S. Bodas, S. Shakkottai, L. Ying, and R. Srikant. Scheduling for Small Delay in Multi-rate Multi-channel Wireless Networks. In Proc. of IEEE INFOCOM, pages 1251-1259, China, 2011.
- [11] J. Qadir, C. Chou, A. Misra, and J. Lim. Minimum Latency Broadcasting in Multiradio, Multichannel, Multirate Wireless Meshes. IEEE Transactions on Mobile Computing, vol.8, no.11, 2009.
- [12] L. Farzinash, and M. Dehghan. Multi-rate Multicast Routing in Multi-gateway Multi-channel Multi-radio Wireless Mesh Networks. (ELSEVIER) Journal of Network and Computer Applications, vol.40, pages 46-60, April 2014.
- [13] R. Cruz. A Calculus for Network Delay, Part I: Network Elements in Isolation. IEEE Transaction on Information Theory, vol.37, no.1, page 114-131, 1991.
- [14] W. Tu. Efficient Resource Utilization for Multi-flow Wireless Multicasting Transmissions. IEEE Journal on Selected Areas in Communications, vol. 30, no. 7, pages 1246-1258, 2012.
- [15] S. Yip, S. Tan, and T. Chuah. Data Rate-Aware Channel Assignment Algorithm For Multi-rate Multi-channel Wireless Mesh Networks. In Proc. of the 6th International Symposium on Wireless and Pervasive Computing, pages 1-6, Hong Kong, 2011.
- [16] G. Zeng, B. Wang, Y. Ding, L. Xiao, and M. Mutka. Efficient Multicast Algorithms for Multichannel Wireless Mesh Networks. IEEE Transactions on Parallel and Distributed Systems, vol.21, no.1, 2010.
- [17] M. Xie, and M. Haenggi. Towards an End-to-end Delay Analysis of Wireless Multihop Networks. Ad Hoc Networks vol.7, issue 5, pages 849861, 2009.
- [18] W. Tu. A Multi-rate Multi-channel Multicast Algorithm in Wireless Mesh Networks. In Proc. of The 39th IEEE Conference on Local Computer Networks (LCN), Canada, 2014.
- [19] B. Awerbuch, D. Holmer, and H. Rubens. High Throughput Route Selection in Multi-Rate Ad Hoc Wireless Networks. Wireless On-demand Network System, Special Issue on "Internet Wireless Access: 802.11 and Beyond", 2004.
- [20] P. Ng, and S. Liew. Throughput Analysis of IEEE 802.11 Multi-Hop Ad Hoc Networks. IEEE/ACM Transactions on Networking, vol.15, no.2, 2007.
- [21] AIRMESH MSR4000 OUTDOOR WIRELESS MESH ROUTER. http://www.arubanetworks.com/pdf/products/DS_MSR4000.pdf
- [22] W. Tu, C. Sreenan, C. Chou, A. Misra, and S. Jha. Resource-Aware Video Multicasting via Access Gateways in Wireless Mesh Network. IEEE Transactions on Mobile Computing, vol. 11, issue 6, pages 881-895, 2012.
- [23] K. Lee, and V. Leung. Utility-Based Rate-Controlled Parallel Wireless Transmission of Multimedia Streams with Multiple Importance Levels. IEEE Transactions on Mobile Computing, vol.8, no.1, January 2009.
- [24] J. Klauke, B. Rathke, and A. Wolisz. EvalVidA Framework for Video Transmission and Quality Evaluation. In Proc. of the 13th International Conference on Modeling Techniques and Tools for Computer Performance Evaluation, pages 255-272, September 2003.



Wanqing Tu is a Reader in the School of Computing Science and Digital Media at the Robert Gordon University (RGU). Before joining RGU, she worked for Glyndwr University and Nottingham Trent University as a Senior Lecturer. She was an IRCSET Embark Initiative Postdoctoral Research Fellow in the Department of Computer Science at University College Cork. She received her PhD from the Department of Computer Science at the City University of Hong Kong. Her research interests include multimedia multicasting, wireless multi-hop

networks, QoS/QoE, large-scale communication technology, mobile computing, distributed computing, etc. She is a senior member of the IEEE.